

Aromatic molecules as spintronic devices

J. H. Ojeda, P. A. Orellana, and D. Laroze

Citation: *The Journal of Chemical Physics* **140**, 104308 (2014); doi: 10.1063/1.4867782

View online: <http://dx.doi.org/10.1063/1.4867782>

View Table of Contents: <http://scitation.aip.org/content/aip/journal/jcp/140/10?ver=pdfcov>

Published by the [AIP Publishing](#)

Articles you may be interested in

[Is spin transport through molecules really occurring in organic spin valves? A combined magnetoresistance and inelastic electron tunnelling spectroscopy study](#)

Appl. Phys. Lett. **106**, 082408 (2015); 10.1063/1.4913908

[Magnetic configuration dependence of magnetoresistance in a Fe-porphyrin-like carbon nanotube spintronic device](#)

Appl. Phys. Lett. **104**, 033104 (2014); 10.1063/1.4862895

[Spintronic transport of a non-magnetic molecule between magnetic electrodes](#)

Appl. Phys. Lett. **103**, 233115 (2013); 10.1063/1.4840176

[Hanle effect missing in a prototypical organic spintronic device](#)

Appl. Phys. Lett. **102**, 092407 (2013); 10.1063/1.4794408

[Molecular spin valve and spin filter composed of single-molecule magnets](#)

Appl. Phys. Lett. **96**, 082115 (2010); 10.1063/1.3319506

A promotional banner for AIP Applied Physics Reviews. On the left is a thumbnail image of a journal cover for "AIP Applied Physics Reviews" featuring a diagram of a device. The main background is blue with a molecular structure of spheres and sticks. The text "NEW Special Topic Sections" is in large white font. Below it, in orange, is "NOW ONLINE" followed by "Lithium Niobate Properties and Applications: Reviews of Emerging Trends". The AIP Applied Physics Reviews logo is in the bottom right.

NEW Special Topic Sections

NOW ONLINE
Lithium Niobate Properties and Applications:
Reviews of Emerging Trends

AIP Applied Physics Reviews

Aromatic molecules as spintronic devices

J. H. Ojeda,^{1,2,a)} P. A. Orellana,³ and D. Laroze¹

¹*Instituto de Alta investigación, Universidad de Tarapacá, Casilla 7D Arica, Chile*

²*Grupo de Física de Materiales, Universidad Pedagógica y Tecnológica de Colombia, Tunja, Colombia*

³*Departamento de Física, Universidad Técnica Federico Santa María, Casilla 110-V, Valparaíso, Chile*

(Received 9 September 2013; accepted 25 February 2014; published online 13 March 2014)

In this paper, we study the spin-dependent electron transport through aromatic molecular chains attached to two semi-infinite leads. We model this system taking into account different geometrical configurations which are all characterized by a tight binding Hamiltonian. Based on the Green's function approach with a Landauer formalism, we find spin-dependent transport in short aromatic molecules by applying external magnetic fields. Additionally, we find that the magnetoresistance of aromatic molecules can reach different values, which are dependent on the variations in the applied magnetic field, length of the molecules, and the interactions between the contacts and the aromatic molecule. © 2014 AIP Publishing LLC. [<http://dx.doi.org/10.1063/1.4867782>]

I. INTRODUCTION

Studies of spin-dependent transport through molecules have been extensively performed in the last decades.^{1–7} These studies include carbon nanotube spin-valves, spin-injection in π -conjugated molecules, and organic tunnel junctions, to mention a few. By considering the direct connection between the conductance and electronic transmission with the possibility to manipulate spins, we can calculate spin-polarized currents.

Theoretical calculations have shown that the electronic current in the molecular system can be substantially affected by changing the magnetic alignment at the contacts or applying a magnetic field in the molecular device.^{8,9} Electrons moving through a non-magnetic material normally have random spins giving a zero net polarization. However, when a magnetic field is applied, spins align allowing new forms of binary storage: ones (all spins up) and zeros (all spins down). This effect was first discovered in a device made of multiple layers of electrically conductive materials and was called as “spin valve” given that its resistance could be controlled by the spin configuration, which in turn is manipulated by external magnetic fields.^{10,11}

One of the devices more used in spintronics, is the magnetic sensor, which consists of a tunnel junction resistance, in which the tunnel magnetoresistance (TMR) or magnetoresistance (MR) effects in organic systems is induced. These effects are originated from the electronic structure of ferromagnetic devices, and have highlighted the importance in the transport properties. In particular, in the possible applications of the storage technology.^{12–18}

The aim of this work is to explore the spin-dependent transport through segments of aromatic molecules. In particular, we study plane segments with one, two, and three benzene aromatic rings placed between two metal contacts. These molecules are modeled using a tight-binding Hamiltonian within a nearest-neighbor approximation described by

Green's functions formalism.^{19–23} By applying an external magnetic field, we study spin-dependent transport in such molecules. Furthermore, we find that benzene molecules display spin valve characteristics even for small values of applied magnetic field.

The paper is organized as follows: In Sec. II, we introduce the model based in a tight binding Hamiltonian for the molecules. In Sec. III, we describe the method utilized. In Sec. IV, we analyze the results. Finally, we summarize the work in Sec. V.

II. MODELS

In order to describe the aromatic molecule as a spintronic device we have adopted three configurations. In particular, we have connected one, two, and three benzene rings, respectively, to the contacts as we see in Figure 1. These configurations are characterized by n carbon atoms, where $n = 6$ for the Benzene molecule (configuration 1) (Fig. 1(a)), $n = 12$ for the Biphenyl molecule (configuration 2) (Fig. 1(b)), and $n = 18$ for the Terphenyl molecule (configuration 3) (Fig. 1(c)).

The full system is described by a tight-binding Hamiltonian, given by

$$H = H_{AR} + H_L + H_I, \quad (1)$$

where H_{AR} corresponds to the Hamiltonian of the aromatic molecule embedded between two electrodes, and is given by

$$H_{AR} = v_c \sum_{i,\sigma} (c_{i\sigma}^\dagger c_{(i+1)\sigma} + c_{(i+1)\sigma}^\dagger c_{i\sigma}) + w \sum_{\sigma} (c_{\alpha\sigma}^\dagger c_{\beta\sigma} + c_{\beta\sigma}^\dagger c_{\alpha\sigma}) + \sum_{i,\sigma} E_{i\sigma} c_{i\sigma}^\dagger c_{i\sigma}, \quad (2)$$

where $c_{i\sigma}^\dagger$ is the creation operator of an electron at site i with spin σ ($\sigma = \uparrow, \downarrow$), v_c is hopping between carbon atoms, w is the hopping between the benzene rings along the molecule and $E_{i\sigma}$ is given by $E_{i\sigma} = E_c + \varepsilon_z$, where E_c is the energy of carbon atom, $\varepsilon_z = g\mu B\sigma$ is the Zeeman energy, B is the

^{a)}Electronic mail: judith.ojeda@uptyc.edu.co

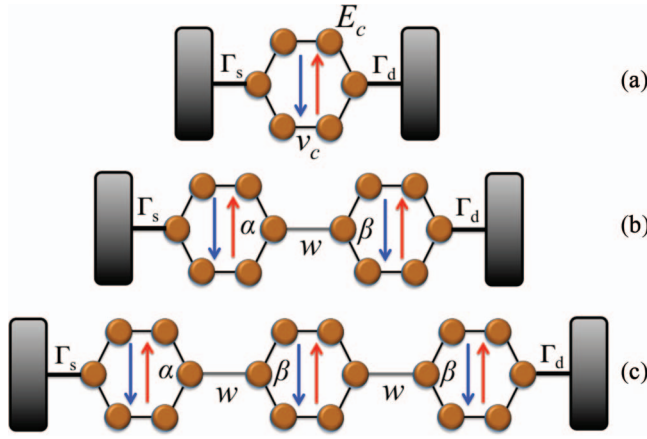


FIG. 1. Aromatic molecules. (a) Benzene molecule (model 1), (b) Biphenyl molecule (model 2), and (c), Terphenyl molecule (model 3).

magnetic field applied perpendicularly to the system (z direction), σ is the Pauli matrix ($\sigma = \sigma_z$), g is the Landé electron factor, and μ is the Bohr magneton.

On the other hand, H_L represents the leads and H_I their interaction with the molecule, given by

$$H_L = \sum_{k_L\sigma} \varepsilon_{k_L\sigma} d_{k_L\sigma}^\dagger d_{k_L\sigma} + \sum_{k_R\sigma} \varepsilon_{k_R\sigma} d_{k_R\sigma}^\dagger d_{k_R\sigma}, \quad (3)$$

$$H_I = \sum_{k_L\sigma} \Gamma_S d_{k_L\sigma}^\dagger c_{1\sigma} + \sum_{k_L\sigma} \Gamma_D d_{k_R\sigma}^\dagger c_{N\sigma} + h.c., \quad (4)$$

where the operator $d_{k_L(R)\sigma}^\dagger$ is the creation operator of an electron in a state $k_L(R)\sigma$ and energy $\varepsilon_{k_L(R)\sigma}$ while $\Gamma_{S(D)}$ is the coupling between each lead with the aromatic molecule.

III. METHOD

We study the spin-dependent transport through aromatic molecules by using the Landauer-Büttiker²⁴⁻²⁶ formalism based on Green's function techniques within a real-space renormalization approach (decimation procedure).^{22,27}

The Green's function of the aromatic molecules coupled to the leads are calculated by using the Dyson equation given by

$$G = G^0 + G^0 (\Sigma_L + \Sigma_R) G, \quad (5)$$

where G^0 is the bare Green's function of the isolated aromatic molecule and Σ_L and Σ_R are the self-energies of the left and right lead, respectively.

The transmission probability can be obtained by using the Fischer-Lee^{25,26} relationship, which is given by

$$T(E) = \text{Tr}[\Gamma^L G^r \Gamma^R G^a], \quad (6)$$

where $\Gamma^{L(R)} = i(\Sigma^{L(R)} - \Sigma^{L(R)\dagger})$ is the spectral matrix density of the left(right) lead, which has non-null elements only for Γ_{11}^L and Γ_{NN}^R , respectively.

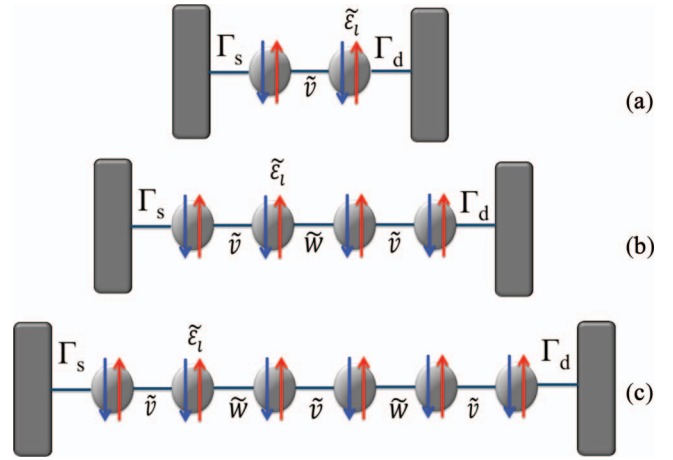


FIG. 2. Effective models: (a) Benzene molecule (model 1), (b) Biphenyl molecule (model 2), and (c) Terphenyl molecule (model 3).

The aromatic molecule representations can be transformed into an effective linear mono-atomic chains, as it is shown in Figure 2.

As we can see, we transform the aromatic molecule representation into an effective one-dimensional chain of sites, obtaining renormalized Green's functions with effective inter-site couplings, which contain all the information of the planar aromatic molecule. Then, the transmission probability can be written as

$$T(E) = \Gamma_{11}^L \Gamma_{NN}^R |G_{1N}^r|^2. \quad (7)$$

The Green's function G_{1N}^0 , G_{NN}^0 , and G_{11}^0 can be analytically determined by using the renormalization techniques, where N represents the effective atomic site. In what follows, we take $\Sigma^L = \Sigma^R = -i\Gamma/2$, and $G_{NN}^0 = G_{11}^0$.

In order to obtain the transmission probability, we determine the Green's functions G_{1N}^0 , G_{11}^0 , and G_{NN}^0 of the effective linear chain for each case, where $N = 2$ for the first configuration, $N = 4$ for the second configuration, and $N = 6$ for the third configuration. These effective chains are characterized by having a corresponding local effective Green's functions ($\tilde{g}_i(E, \sigma) = 1/(E - \tilde{\varepsilon}_i(E, \sigma))$), where the effective energy $\tilde{\varepsilon}_i(E, \sigma)$ is given by

$$\tilde{\varepsilon}_i(E, \sigma) = E - \left\{ \frac{(E - E_{i\sigma})^2 - 3v_c^2}{E - E_{i\sigma} + 2v_c - \frac{v_c^2}{E - E_{i\sigma}}} \right\}. \quad (8)$$

The effective couplings ($\tilde{v}(E, \sigma)$, $\tilde{w}(E, \sigma)$) are given by

$$\tilde{v}(E, \sigma) = \frac{2v_c^3}{(E - E_{i\sigma})^2 + 2v_c(E - E_{i\sigma}) - v_c^2}, \quad (9)$$

$$\tilde{w}(E, \sigma) = \frac{w((E - E_{i\sigma})^2 - v_c^2)}{(E - E_{i\sigma})^2 + 2v_c(E - E_{i\sigma}) - v_c^2}. \quad (10)$$

Then we can rewrite Eq. (7) for the three configurations as

$$T_\sigma(E) = \frac{16\lambda(1 - \Lambda)}{(4\Lambda - \lambda)^2 + 16\lambda}, \quad (11)$$

where $\lambda = (\Gamma \tilde{g}_i)^2$ and $\Lambda = 1 - (\tilde{g}_i \tilde{v})^2$,

$$T_\sigma(E) = \frac{16\lambda\Upsilon^2(1-\Lambda)^2}{[(4(\Lambda^2 - \Upsilon^2) - \lambda(1 - \Upsilon^2))^2 + 16\lambda(1 - \Upsilon^2)^2]}, \quad (12)$$

where $\Upsilon = \tilde{g}_i \tilde{w}$,

$$T_\sigma(E) = \frac{16\lambda\alpha^2\Upsilon^4(1-\Lambda)^3}{[4\alpha^2 - \lambda(\eta^2 - \Upsilon^4(1-\Lambda)^3)]^2 + 16\lambda\eta^2\alpha^2}, \quad (13)$$

where $\alpha = \Lambda^3 - 2\Upsilon^2\Lambda + \Upsilon^4$ and $\eta = \Lambda^2 - \Upsilon^2(1 - \Upsilon^2 + \Lambda)$.

Equations (11)–(13) are the probability transmission for the configurations 1, 2, and 3, respectively.

The transmission through the aromatic molecules can be considered as a one-dimensional scattering process of an electron between the leads. Using the Landauer formalism, the I - V characteristics can be obtained by the following expression:^{25,26}

$$I_\sigma(V) = I_0 \int_{-\infty}^{\infty} (f_L - f_R) T_\sigma(E) dE, \quad (14)$$

where $I_0 = 2e/h$. $f_{L(R)}$ is the Fermi-Dirac distribution function given by

$$f_{L(R)} = \frac{1}{1 + \exp(\beta(E - \mu_{L(R)}))}, \quad (15)$$

such that β is the Boltzmann's factor and $\mu_{L(R)} = E_f \pm eV/2$ is the chemical potential. Note that in the limit of zero bias (or zero temperature) Eq. (14) is reduced to²⁶

$$I_\sigma(V) = I_0(\mu_L - \mu_R) T_\sigma(E_f). \quad (16)$$

For the sake of simplicity we have assumed that the bias voltage drops at the aromatic molecule-lead interfaces. This assumption does not affect the qualitative behavior of the I - V characteristics of these molecular systems.

Let us introduce the MR , which is defined as a relative change of the current of system when the magnetized currents switch between the current with spin-up and spin-down. The MR can be expressed as^{17,18}

$$MR = \frac{I_{\uparrow,\downarrow} - I_{(B=0)}}{I_{(B=0)}}, \quad (17)$$

where I_\uparrow and I_\downarrow are the currents with spin-up (or) and spin-down, respectively, generated by the application of an external magnetic field in direction perpendicular to the growth of the molecule. Here, $I_{(B=0)}$ represents the current without magnetic field.

IV. RESULTS

We analyze the coherent spin-dependent transport through of the aromatic molecules, by considering three different configurations: Benzene molecule, Biphenyl molecule, and Terphenyl molecule, characterized by having one, two, or three benzene rings, respectively (Figure 1). By varying Γ and B , we can calculate the transport properties taking into account the spin, which is the basis of spintronics devices. Such effect has been studied extensively in several

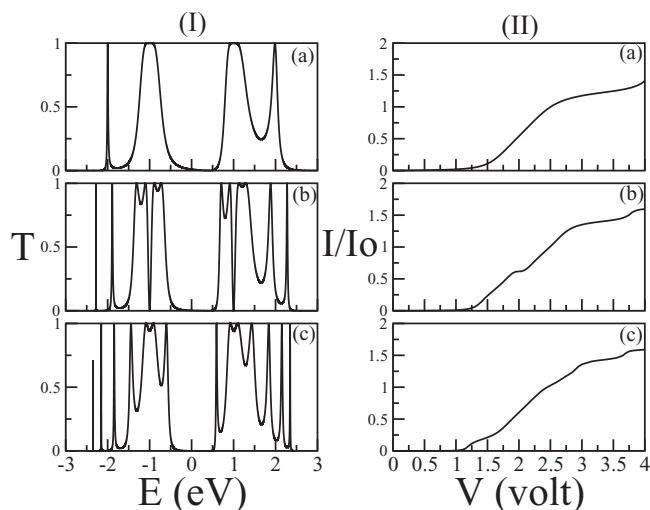


FIG. 3. Probability transmission (Panel I) and current vs. voltage (Panel II) for (a) Benzene molecule, (b) Biphenyl molecule, and (c) Terphenyl molecule. The fixed parameters are $\Gamma = 0.1$ eV, $T = 0$ K, $E_c = 0$ eV, $v_c = 1$ eV, and $B = 0$.

works.^{7,28–31} In what follows, we have considered the temperature $T = 0$ K, the on-site energy $E_c = 0$ eV, the inter-site potential $v_c = 1$ eV, and the inter-ring hopping $w = v_c$.³² We remark that, this set of molecular parameters is into the range of the parameters used to obtain the results calculated by Kondo *et al.*³³ using the non-equilibrium Green's function method based on the density functional theory (DFT). Besides these are consistent with the experimental results given by Kirchner *et al.*³⁴ In addition, to complement our study, we will explore other sets of molecular parameters which have been calculated using DFT.^{35–38}

Results of the transmission probability as a function of energy and current as function of voltage are displayed in the Panel I and the Panel II of Fig. 3, respectively. From the transmission probability we observe that the systems are in resonant tunnelling regime. Therefore, unitary transmission peaks are displayed, one for each atomic site in the molecule. These resonant peaks are associated with the eigenvalues of each aromatic molecule. Also, we can observe that the bandwidth in the transmission probability is $2v_c$ in all configurations, which is in agreement with the results of Maiti.³²

In the characteristics curves of current-voltage (Panel II) we observe that when the number of rings grows the current amplitude increases smoothly. Few small steps associated resonances can be also observed, such that the number of steps increases when the length in the aromatic compound increases too. Another important fact is that the gap of the voltage is the same for all systems ($V \sim 1.2$ V) which is in agreement with the results of Mojtaba *et al.*⁶

Figure 4 shows a contour plot of the transmission versus E and ε_z of a Benzene molecule for both spin states. We remark that the displacement of the transmission bands grow apart as the magnetic field increases. Also, we can observe that the internal structure of the bands have opposite slopes, and are qualitatively different.

Figure 5 shows MR as a function of the bias voltage for the three aromatic molecules. In this figure, the spin-up and

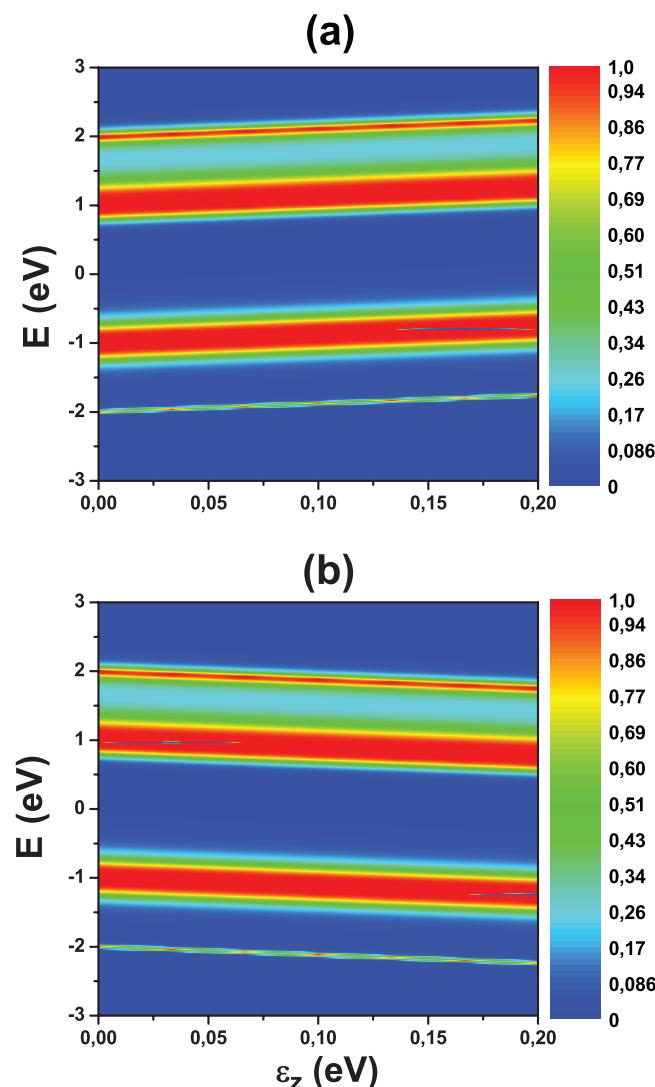


FIG. 4. Contour plot of the transmission probability as function of energy and ε_z for the Benzene molecule. (a) Spin down and (b) spin up. The fixed parameters are $\Gamma = 0.1$ eV, $T = 0$ K, $E_c = 0$ eV, and $v_c = 1$ eV.

the spin-down are represented by (blue) up-triangles and (red) down-triangles, respectively. The MR is originated by the difference between currents of different spins, as it is shown in Eq. (17). In all the cases, the MR behaves such that the current amplitude with spin-down is less than the amplitude of the current with spin-up, until a point where the both currents coincide, and after this critical point the behavior is inverted. This issue occurs because the bands with spin-up are almost full while the others are almost unoccupied. Therefore, bands with spin-up have a lower probability that the electrons pass through the sample.

At zero bias ($V = 0$) the value of the MR is the same for the (b) and (c) configurations, which is ($MR \sim 0.4\%$). When the number of aromatic rings in each molecule increases, the maximum (minimum) value of MR increases. This scenario is given by the strong coupling regime in which the molecule is placed. Hence, the contact states hybridize with the states of the molecule through the exchange of an electron or hole between the metal and the neutral molecule, which is in concordance with the results obtained by Walczak.³⁹

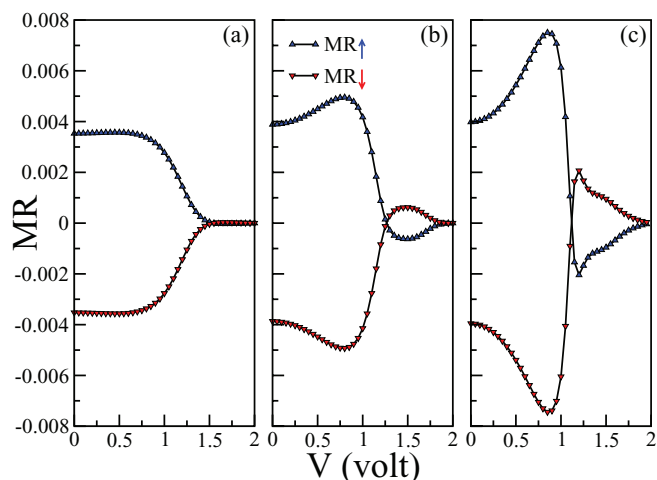


FIG. 5. MR as a function of bias voltage for (a) Benzene molecule, (b) Biphenyl molecule, and (c) Terphenyl molecule. The with spin-up and spin-down are represented by (blue) up-triangles and with (red) down-triangles, respectively. The fixed parameters are $\Gamma = 0.5$ eV, $T = 0$ K, $E_c = 0$ eV, $v_c = 1$ eV, and $\varepsilon_z = 100$ μ eV.

We emphasize that the voltage needed for both polarized currents coincide diminishes with the growth of size the molecular device. So, the width of the profile in the MR is lesser for systems containing larger number of benzene rings as it is shown in Figure 5.

The panel I of Figure 6 displays the MR with spin-up as a function of the voltage bias for different values of the magnetic field at a fixed value of molecule-lead coupling, $\Gamma = 0.5$ eV, in the case of Benzene (frame (a)), Biphenyl (frame (b)), and Terphenyl (frame (c)). Notice that the maximum of MR increases with the magnetic field. Also, we can observe for Biphenyl and Terphenyl that the MR has negative values when the voltage increases, chaining the polarization. Moreover, the MR ratio increases with the size of aromatic molecule until approximately 0.4%.

The panel II of Figure 6 shows the dependence of voltage on the MR for the three molecules with different values

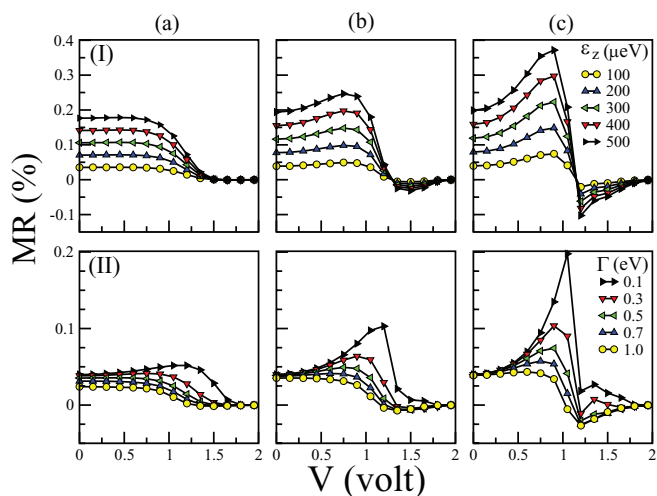


FIG. 6. MR varying field (panel I) and MR varying molecule-leads coupling Γ (panel II) for (a) Benzene molecule, (b) Biphenyl molecule, and (c) Terphenyl molecule.

of Γ at a fixed magnetic field, $\varepsilon_z = 100 \mu\text{eV}$. We find two coupling regimes: weak coupling ($\Gamma \ll v_c$) and a strong coupling ($\Gamma \geq v_c$). In the case of weak coupling limit, the magnetoresistance takes large values of MR in all the molecules. Nonetheless, for strong coupling regime, the MR exhibits a valley, which is reduced to constant value as it is clearly shown in the Benzene.

From our results we can infer that the magnetoresistance can be modified by the device operating conditions, such as the molecule-lead coupling, the magnetic field and the bias voltage. Hence, this system is affected by a spin-transfer-torque. When the electrons inside from a non-ferromagnetic contact (source) to the molecule, they will align in the direction of the external field applied to the molecular system, at the time when the electron come into contact (drain). At the interface scattering events occur causing the attenuation of the electrons energy. For this reason, the molecule-contact interface acts as a spin filter, and generates a magnetoresistance.

Finally, let us study the effect the temperature, Θ , on the MR . Figure 7 depicts the MR as a function of voltage for four temperature values in the range of 0–300 K in the case of the Biphenyl molecule. The continue lines are for the MR with spin up, while the dashed lines are for the MR with spin down. The profile of the MR shows that it is almost same for four temperature values when the values of the voltage is small. Only slightly variations can be found in the intermediate range of voltage as it is shown the inset of the aforementioned figure. Therefore, we can say that the MR is essentially independent of the temperature in these molecular systems.

The MR calculated for the three organic molecular systems listed in this paper, can be called also as organic magnetoresistance. This effect has been found in a wide variety of organic semiconducting small molecules and polymers and could be used for magnetic pen input displays or large area magnetic field sensors.^{17,18,40}

In order to investigate deeply how the molecular structure affect the transport properties, let us analyze other two set of molecular parameters based on the works of Pauly *et al.*³⁵ and

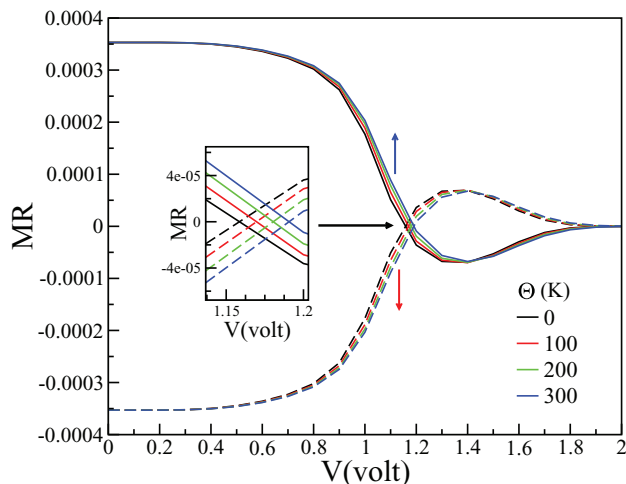


FIG. 7. MR for the Biphenyl molecule varying temperature Θ for $\Gamma > v_c$, $\varepsilon_z = 100 \mu\text{eV}$. Spin up (continue lines) and spin down (dashed lines).

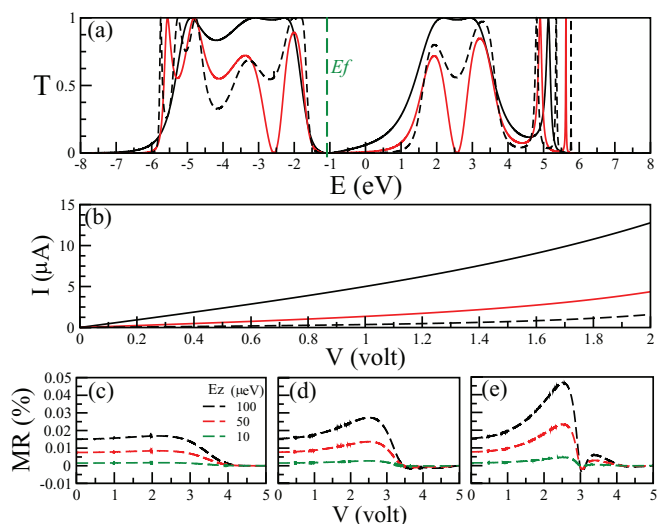


FIG. 8. (a) Transmission probability for the Benzene molecule (black line), Biphenyl molecule (red line), and Terphenyl molecule (black dashed line), (b) Current as function voltage for the same molecules given in Figure 1(a), (c) Magneto-resistance, MR , for the Benzene molecule, (d) MR for the Biphenyl molecule, and (e) MR for the Terphenyl molecule. The fixed parameters are: $E_c = 0 \text{ eV}$, $v_c = -2.57 \text{ eV}$, and $\Gamma = 0.64 \text{ eV}$.

Bürkle *et al.*^{37,38} Figure 8 shows the transmission probability as a function of the energy (frame (a)), the current as function of the voltage (frame (b)), and the Magneto-resistance as a function of the voltage (frame (c)) for Benzene, Biphenyl, and Terphenyl molecules with the following set of parameters: $E_c = 0 \text{ eV}$, $v_c = -2.57 \text{ eV}$, and $\Gamma = 0.64 \text{ eV}$.³⁵ Note that we numerically found that the Fermi energy ($E_f \sim -1.08 \text{ eV}$) is almost the same value than the corresponding value given by Pauly *et al.*³⁵ Also, we found that the amplitude of MR has the same order of magnitude of the experimental work of Li *et al.*,⁴¹ which is: 0.01% to 0.04%.

In Figure 9, we show the same plots for Biphenyl molecule, but the molecular parameters are taken from the work of Bürkle *et al.*,^{37,38} which are explicitly:

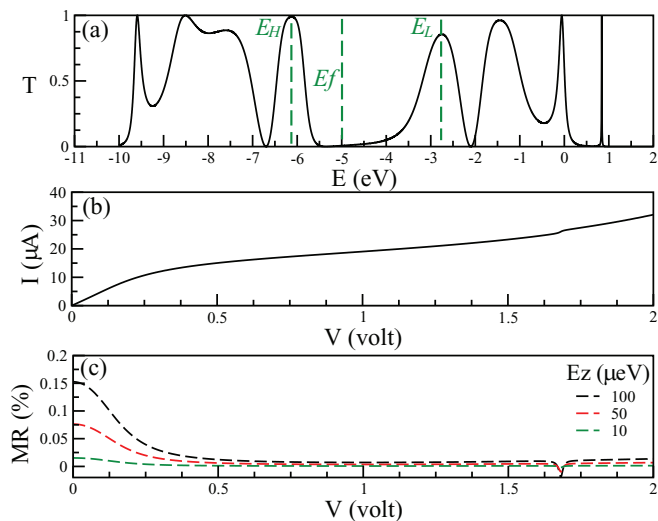


FIG. 9. (a) Transmission probability, as a function of the energy; current (b); and MR (c), as function of the voltage for the Biphenyl molecule. The fixed parameters are: $E_c = -4.40 \text{ eV}$, $v_c = -2.30 \text{ eV}$, and $\Gamma = 0.70 \text{ eV}$.

$E_c = -4.40$ eV, $v_c = -2.30$ eV, and $\Gamma = 0.70$ eV. In this case, we also found that the energies are almost the same than the given by the authors. Respect to the MR in this case we found that it is in the range of 0.01% to 0.15%, which is also in the correct order of magnitude of the experimental data.⁴¹

V. CONCLUSIONS

In this paper, we have studied the coherent spin-dependent transport through aromatic molecules by adopting three different configurations. We model the system by a nearest neighbor tight-binding approach Hamiltonian. By using Green's function techniques within a real-space renormalization scheme, we have calculated the transmission probability, the I - V characteristics, and the magnetoresistance for each finite aromatic molecule coupled to two semi-infinite leads. These properties have been studied as a function of molecule-leads coupling parameters and applied magnetic field. For a fixed value of molecule-lead coupling, we found that MR depends on the size of the molecule, and it increases as the magnetic field is increased. Hence, we have shown that spin-filter properties can be found on aromatic system. To analyze different scenarios, we have calculated with three different types of molecular parameters, the first one corresponding to the obtained by non-equilibrium Green's functions^{32,33} and verified experimentally;³⁴ and the other two set calculated by DFT method.^{35,37} It should be also mentioned that the alignment of the electrode's magnetization is due to the external magnetic field within the molecular region. This can have a direct effect in the shape of the conductance considering a shift of the bands in the transmission probability. The structure molecular offered by organic materials as in the present setup could enable the use in spintronic devices.^{41,42}

ACKNOWLEDGMENTS

J.H.O. acknowledges the financial support from FONDECYT Postdoctoral program fellowship under Grant No. 3130506. P.A.O. acknowledges the financial support from FONDECYT under Grant No. 1100560. D.L. acknowledges partial financial support from FONDECYT 1120764, Millennium Scientific Initiative, P10-061-F, Basal Program Center for Development of Nanoscience and Nanotechnology (CEDENNA), and UTA-project 8750-12.

¹B. Zhao, I. Mönch, H. Vinzelberg, T. Mühl, and C. M. Schneider, *Appl. Phys. Lett.* **80**, 3144 (2002).

²V. Dediu, M. Murgia, F. C. Matocotta, C. Taliani, and S. Barbanera, *Solid State Commun.* **122**, 181 (2002).

³Z. H. Xiong, D. Wu, Z. Valy Vardeny, and J. Shi, *Nature (London)* **427**, 821 (2004).

- ⁴J. R. Petta, S. K. Slater, and D. C. Ralph, *Phys. Rev. Lett.* **93**, 136601 (2004).
- ⁵J. H. Wei, X. J. Liu, S. J. Xie, and YiJing Yan, *J. Chem. Phys.* **131**, 064906 (2009).
- ⁶A. Mojtaba, S. Nasser, V. Davoud, and A. Mostafa, *J. Phys.: Conf. Ser.* **248**, 012045 (2010).
- ⁷F. Wang and Z. Valy Vardeny, *Synth. Met.* **160**, 210 (2010).
- ⁸E. G. Emberly and G. Kirczenow, *Chem. Phys.* **281**, 311 (2002).
- ⁹R. Pati, M. Mailman, L. Senapati, P. M. Ajayan, S. D. Mahanti, and S. K. Nayak, *Phys. Rev. B* **68**, 014412 (2003).
- ¹⁰L. Bogani and W. Wernsdorfer, *Nat. Mater.* **7**, 179 (2008).
- ¹¹V. M. García-Suárez, J. Ferrer, and C. J. Lambert, *Phys. Rev. Lett.* **96**, 106804 (2006).
- ¹²A. R. Rocha, V. M. García-Suárez, S. W. Bailey, C. J. Lambert, J. Ferrer, and S. Sanvito, *Nat. Mater.* **4**, 335 (2005).
- ¹³S. Krompiecki, *Phys. Status Solidi B* **242**, 226 (2005).
- ¹⁴D. Liu, Y. Hu, H. Guo, and X. F. Han, *Phys. Rev. B* **78**, 193307 (2008).
- ¹⁵J. Woo Yoo, H. W. Jang, V. N. Prigodin, C. Kao, C. B. Eom, and A. J. Epstein, *Synth. Met.* **160**, 216 (2010).
- ¹⁶D. Sun, L. Yin, C. Sun, H. Guo, Z. Gai, X. G. Zhang, T. Z. Ward, Z. Cheng, and J. Shen, *Phys. Rev. Lett.* **104**, 236602 (2010).
- ¹⁷J. D. Bergeson, V. N. Prigodin, D. M. Lincoln, and A. J. Epstein, *Phys. Rev. Lett.* **100**, 067201 (2008).
- ¹⁸F. J. Wang, H. Bässler, and Z. Valy Vardeny, *Phys. Rev. Lett.* **101**, 236805 (2008).
- ¹⁹M. Dey, S. K. Maiti, and S. N. Karmankar, *Org. Electron.* **12**, 1017 (2011).
- ²⁰L.-Y. Hsu and B.-Y. Jin, *Chem. Phys. Lett.* **457**, 279 (2008).
- ²¹K. Walczak, *Phys. Status Solidi B* **241**, 2555 (2004).
- ²²J. H. Ojeda, M. Pacheco, L. Rosales, and P. A. Orellana, *Org. Electron.* **13**, 1420 (2012).
- ²³J. H. Ojeda, R. R. Rey-Gonzalez, and D. Laroze, *J. Appl. Phys.* **114**, 213702 (2013).
- ²⁴Y. M. Blanter and M. Büttiker, *Phys. Rep.* **336**, 1 (2000).
- ²⁵S. Datta, *Electronic Transport in Mesoscopic Systems* (Cambridge University Press, Cambridge, 1997).
- ²⁶M. Di Ventra, *Electrical Transport in Nanoscale System* (Cambridge University Press, Cambridge, 2008).
- ²⁷M. Nardelli, *Phys. Rev. B* **60**, 7828 (1999).
- ²⁸H. Dalglish and G. Kirczenow, *Phys. Rev. B* **72**, 184407 (2005).
- ²⁹A. Saffarzadeh, *J. Appl. Phys.* **104**, 123715 (2008).
- ³⁰J. H. Ojeda and P. A. Orellana, *J. Supercond. Novel Magn.* **26**, 2227 (2013).
- ³¹D. Rai, O. Hod, and A. Nitzan, *Phys. Rev. B* **85**, 155440 (2012).
- ³²S. K. Maiti, *Eur. Phys. J. B* **86**, 296 (2013).
- ³³H. Kondo, J. Nara, H. Kino, and T. Ohno, *J. Chem. Phys.* **128**, 064701 (2008).
- ³⁴T. Kirchner, B. Briechele, E. Scheer, J. Wolf, T. Huhn, and A. Erbe, *Acta Phys. Pol., A* **121**, 410 (2012), available online at http://yadda.icm.edu.pl/przyrbwn/element/bwmeta1.element.bwnjournal-article-appv121n255kz?q=4a04db02-2f64-4c70-aedb-f97641c69c5f&qt=IN_PAGE.
- ³⁵F. Pauly, J. K. Viljas, and J. C. Cuevas, *Phys. Rev. B* **78**, 035315 (2008).
- ³⁶F. Pauly, J. K. Viljas, J. C. Cuevas, and G. Schön, *Phys. Rev. B* **77**, 155312 (2008).
- ³⁷M. Bürkle, J. K. Viljas, D. Vonlanthen, A. Mishchenko, G. Schön, M. Mayor, T. Wandlowski, and F. Pauly, *Phys. Rev. B* **85**, 075417 (2012).
- ³⁸M. Bürkle, L. A. Zotti, J. K. Viljas, D. Vonlanthen, A. Mishchenko, T. Wandlowski, M. Mayor, G. Schön, and F. Pauly, *Phys. Rev. B* **86**, 115304 (2012).
- ³⁹K. Walczak, "Tunnel magnetoresistance of polymeric chains," e-print [arXiv:cond-mat/0410625](http://arxiv.org/abs/cond-mat/0410625).
- ⁴⁰F. L. Bloom, W. Wagemans, M. Kemerink, and B. Koopmans, *Phys. Rev. Lett.* **99**, 257201 (2007).
- ⁴¹B. Li, C.-Y. Kao, J.-W. Yoo, V. N. Prigodin, and A. J. Epstein, *Adv. Mater.* **23**, 3382 (2011).
- ⁴²K. Ando, S. Watanabe, S. Mooser, E. Saitoh, and H. Sirringhaus, *Nat. Mater.* **12**, 622 (2013).